Photoinduced Charge Separation Involving an Unusual Double Electron Transfer Mechanism in a Donor−Bridge−Acceptor Molecule

Scott E. Miller, Aaron S. Lukas, Emily Marsh, Patrick Bushard, and Michael R. Wasielewski*

Contribution from the Department of Chemistry, Northwestern University, Evanston, Illinois 60208-3113

Received April 13, 2000

Abstract: A series of rodlike donor−bridge−acceptor (D−B−A) molecules was synthesized to study the role of bridge energy levels on electron transfer (ET) rates. In these compounds, a 4-aminonaphthalene-1,8-imide (ANI) electron donor is linked to a 1,8:4,5-naphthalenediimide acceptor (NI) via the 1,4 positions on a phenyl bridge. The phenyl bridge is substituted at the 2 and 5 positions with methyl or methoxy groups to yield ANI-diMe-NI and ANI-diMeO-NI. These molecules differ only in the energy levels of the bridge molecular orbitals. Other parameters affecting ET rates such as donor−acceptor distance, orientation, and driving force are constant between the two systems. The rate constants for charge separation (CS) and charge recombination (CR) within ANI-diMeO-NI in toluene are 32 and 1400 times larger, respectively, than the corresponding rate constants for ANI-diMe-NI. Solvents of higher polarity diminish these differences in rate constants, making them comparable to those observed for ANI-diMe-NI. The relative energies of the ion pair states suggest that it is possible for the reaction ^{1}*D−B−A → D−B$^+$−A$^-$ to occur via a double electron-transfer process that is somewhat analogous to Dexter energy transfer. The lowest excited singlet state of the donor, ^{1}*ANI, possesses about 70% charge-transfer character, so that significant positive charge is localized on its amine nitrogen, whereas significant negative charge is localized on its naphthalene-1,8-imide ring. Electron transfer from the naphthalene-1,8-imide ring of ^{1}*ANI to NI is concomitant with electron transfer from the *p*-dimethoxybenzene bridge to the electron-deficient amine nitrogen atom in ^{1}*ANI. A series of reference molecules in which the *p*-dimethoxybenzene bridge moiety is attached only to ANI or NI alone is used to establish the structural and electronic requirements for this unusual charge separation mechanism.

Introduction

The bacterial photosynthetic reaction center has been studied extensively due to its ability to convert light energy into chemical energy with near-unity quantum yield.[1] The initial events of charge separation consist of electron transfer (ET) from the initially excited bacteriochlorophyll dimer (P) to the bacteriopheophytin (H) over a distance of 17 Å in 3 ps. The mechanism of this electron transfer is of particular interest, and has been studied to determine the function of the intermediary bacteriochlorophyll (BChl) that is positioned between P and H.[2−6] Discussions in the literature center on whether a two-step, sequential electron transfer occurs, yielding the intermediate P$^+$−BChl$^-$−H, or whether the BChl participates indirectly via a superexchange mechanism.[7−10]

In a typical donor−bridge−acceptor molecule (D−B−A) the superexchange mechanism for electron transfer involves mixing of electronic states of the bridge molecule with those of the donor and acceptor. This mixing depends critically on both the spatial overlap of the molecular orbitals of B with those of D and A and the vertical energy gap between ^{1}*D−B−A and the energetically higher lying D$^+$−B$^-$−A state.[11] In principle, several different states of the bridge molecule can contribute to the overall electronic coupling between the donor and the acceptor, their relative contributions being determined by the electronic couplings and the energy gaps between the various states.[12−14] In addition to P$^+$−BChl$^-$−H, several other states have been invoked in an attempt to describe the primary ET step in the reaction center. Bixon et al. analyzed femtosecond spectroscopic data on the reaction center assuming that the sequential and superexchange mechanism operate competitively.[5] The relative contributions of the two mechanisms were found to depend on the energy gap between the initial ^{1}*P−BChl−H state and the intermediate P$^+$−BChl$^-$−H state. The authors suggested that the presence of the two mechanisms

* Address correspondence to this author. E-mail: wasielew@chem.nwu.edu.

(1) Deisenhofer, J.; Epp, O.; Miki, K.; Huber, R.; Michel, H. *J. Mol. Biol.* **1984**, *180*, 385−398.
(2) Kirmaier, C.; Holten, D. *Proc. Natl. Acad. Sci. U.S.A.* **1990**, *87*, 3552−3556.
(3) Holzapfel, W.; Finkele, U.; Kaiser, W.; Oesterhelt, D.; Scheer, H.; Stilz, H. U.; Zinth, W. *Chem. Phys. Lett.* **1989**, *160*, 1−7.
(4) Martin, J. L.; Breton, J.; Hoff, A. J.; Migus, A.; Antonetti, A. *Proc. Natl. Acad. Sci. U.S.A.* **1986**, *83*, 957.
(5) Bixon, M.; Jortner, J.; Michel-Beyerle, M. E. *Biochim. Biophys. Acta* **1991**, *1056*, 301−315.
(6) Kirmaier, C.; Holten, D. *Electron Transfer and Charge Recombination Reactions in Wild-Type and Mutant Bacterial Reaction Centers*; Deisenhofer, J., Norris, J. R., Eds.; Academic Press: San Diego, 1993; Vol. 2, pp 49−71.
(7) Ogrodnik, A.; Michel-Beyerle, M. E. *Z. Naturforsch.* **1989**, *44a*, 763−764.
(8) DiMagno, T. J.; Norris, J. R. *Initial Electron-Transfer Events in Photosynthetic Bacteria*; Deisenhofer, J., Norris, J. R., Eds.; Academic Press: San Diego, 1993; Vol. 2, pp 105−133.
(9) Sumi, H.; Kakitani, T. *Chem. Phys. Lett.* **1996**, *252*, 85−93.
(10) Plato, M.; Mobius, K.; Michel-Beyerle, M. E.; Bixon, M.; Jortner, J. *J. Am. Chem. Soc.* **1988**, *110*, 7279−7285.
(11) McConnell, H. M. *J. Chem. Phys.* **1961**, *35*, 508−515.
(12) Kuznetsov, A. M.; Ulstrup, J. *J. Chem. Phys.* **1981**, *75*, 2047−2055.
(13) Tang, J.; Wang, Z.; Norris, J. R. *J. Chem. Phys.* **1993**, *99*, 979−984.
(14) Tang, J.; Norris, J. R. *J. Chem. Phys.* **1994**, *101*, 5615−5622.

10.1021/ja001298w CCC: $19.00 © 2000 American Chemical Society
Published on Web 07/28/2000

provide redundancy, which allows efficient charge separation under many different conditions. Won and Friesner[15] suggested that the initial excited state mixes strongly with a charge resonance state of the special pair dimer, increasing the superexchange coupling. Fischer proposed that the involvement of a virtual oxidized bridge state, $P-BChl^{+}-H^{-}$, is consistent with the energies of the reaction center chromophores,[16] and further proposed a real state called the "trip−trip singlet" in which triplet states on both P and the intermediate BChl interact in what is formally a singlet state.[17] More recently, Sumi and Kakatani have suggested that a more useful approach would be to describe bridge-mediated ET as a single, unique process rather than attempting to characterize the relative contributions of sequential ET versus superexchange.[9]

Several D−B−A systems have been synthesized and used as experimental tests of superexchange. Sessler and co-workers synthesized a series of triads consisting of two porphyrins and a quinone bonded in various orientations.[18] This group was able to adjust the ion pair state energies of the bridging porphyrin via selective metalation of one of the two macrocycles. Photoinduced charge separation (CS) occurred in these Zn porphyrin-quinone dyads on time scales of ≤1 ps, while thermal charge recombination (CR) occurred in 3−6 ps. In free-base porphyrin−zinc porphyrin−quinone (HP−ZnP−Q) triads, excitation of ZnP formed a transient species whose 55−75 ps lifetime showed little temperature dependence. This species was identified as the $HP^{+}-ZnP-Q^{-}$ ion pair formed by the superexchange mechanism.

Warman, Paddon-Row, and Verhoeven examined the distance dependence of photoinduced ET through norbornyl bridges of varying length in an extensive series of D−B−A molecules.[19,20] In addition, ester groups were added to the bridge molecules in an attempt to adjust their orbital energies. However, no effect was observed on the rates for either charge separation or recombination. Unusually fast charge recombination was seen in a triad of the form D_2-D_1-A, which undergoes two-step CS to yield the giant-dipole state $D_2^{+}-D_1-A^{-}$.[21] The observed rapid CR reaction was rationalized in the context of a superexchange mechanism involving $D-B^{+}-A^{-}$ virtual states. The competition between sequential vs superexchange charge recombination was also considered in a series of triads studied by the same group.[22]

Gust, Moore, and Moore have addressed the role of superexchange in a series of carotenoid−porphyrin−quinone triads.[23] The ET rate was observed to decrease when rotation about a single bond linking the porphyrin and quinone was hindered by the steric influence of adjacent methyl groups. Furthermore, the direction of the amide linkage between the porphyrin donor and quinone acceptor demonstrated a larger, almost 30-fold effect on the ET rates in these systems.

Wasielewski et al.[24] have addressed the effects of changing both structural isomers and the energy levels of the bridging molecule. Several compounds were examined which employ a pentiptycene spacer between a ZnP donor and a 1,4-naphthoquinone acceptor. Addition of two methoxy groups to the central benzene ring of the pentiptycene spacer did not change the rate of CS, but produced a 3- to 4-fold increase in the CR rate. By comparing the intermediate state energies for the unsubstituted and methoxy-substituted bridge molecules, the $D-B^{+}-A^{-}$ state was suggested as the virtual state that mediates the fast CR reaction.

A series of chlorophyll−porphyrin−quinone triads that use zinc chlorophylls as the primary electron donor has also been studied.[25,26] The bridge species is either a zinc or free-base porphyrin and the electron acceptor moiety is a triptycene-1,4-naphthoquinone. A comparison of the ET rates in compounds with a ZnP bridge to those with the corresponding HP bridge shows that the CS and CR rates increase 11- and 3-fold, respectively, when the ZnP bridge is used. These effects were observed despite the fact that HP is approximately 0.25 V easier to reduce than ZnP. These results flatly contradict the expected behavior if a $D^{+}-B^{-}-A$ virtual state mediates the CS reaction. On the other hand, the data are consistent with the possible involvement of a virtual $D-B^{+}-A^{-}$ state in this reaction, based on the corresponding relative ease of oxidation of the bridge molecule.

Osuka et al. synthesized several multicomponent chlorophyll and porphyrin systems in an effort to model the photosynthetic RC.[27,28] Chlorophyll−porphyrin−pyromellitimide (ZC−HP−PI) triads, similar to the structures of Johnson et al.,[25] were studied in which phenyl rings separated each of the components and pyromellitimide (PI) was the acceptor. In these systems superexchange was ruled out as the CS mechanism based on the similarity between the photophysical behavior of the ZC−HP−PI triad and the ZC−HP dyad. When the bridge molecule is HP, sequential CS results: $^{1}*ZC-HP-PI \rightarrow ZC^{+}-HP^{-}-PI \rightarrow ZC^{+}-HP-PI^{-}$. This mechanism was confirmed by direct observation of the HP anion radical by transient absorption spectroscopy. In an extension of this work, a 1,2-phenylene-bridged ZnP dimer (D) was used as the primary chromophore in an attempt to mimic the dimeric electron donor in the RC. A superexchange mechanism for CR was implicated in the D−HP−PI triad as evidenced by the biexponential decay of $D^{+}-HP-PI^{-}$, in which one of the decay components displayed no temperature dependence. Another compound, D−ZnP−PI, exhibited CS in 500 ps in THF, yielding the distal ion pair $D^{+}-ZnP-PI^{-}$. Unlike other compounds in this study, the reduced state of the bridge was not detected, leading the researchers to conclude that the electron transfer was superexchange-mediated.

Zimmt et al. have extended studies of superexchange in structurally well-defined systems to include electron transfer through trapped solvent in a series of C-clamp molecules.[29] These molecules are based on extended polycyclic norbornyl

(15) Won, Y.; Friesner, R. A. *Biochim. Biophys. Acta* **1988**, *935*, 9−18.
(16) Fischer, S. F.; Scherer, P. O. J. *Chem. Phys.* **1987**, *115*, 151−158.
(17) Fischer, S. F.; Scherer, P. O. J. *Eur. Biophys. J.* **1997**, *26*, 477−483.
(18) Sessler, J. L.; Johnson, M. R.; Lin, T.-Y. *Tetrahedron* **1989**, *45*, 4767−4784.
(19) Verhoeven, J. W. *Adv. Chem. Phys.* **1999**, *106*, 603−644.
(20) Warman, J. M.; Smit, K. J.; de Haas, M. P.; Jonker, S. A.; Paddon-Row, M. N.; Oliver, A. M.; Jan, K.; Oevering, H.; Verhoeven, J. W. *J. Phys. Chem.* **1991**, *95*, 1979−1987.
(21) van Dijk, S. I.; Wiering, P. G.; van Staveren, R.; van Ramesdonk, H. J.; Brouwer, A. W.; Verhoeven, J. W. *Chem. Phys. Lett.* **1993**, *214*, 502−506.
(22) Roest, M. R.; Lawson, J. M.; Paddon-Row, M. N.; W., V. J. *Chem. Phys. Lett.* **1994**, *230*, 536−542.
(23) Kuciauskas, D.; Liddell, P. A.; Hung, S.-C.; Lin, S.; Stone, S.; Seely, G. R.; Moore, A. L.; Moore, T. A.; Gust, D. *J. Phys. Chem. B* **1997**, *101*, 429−440.
(24) Wasielewski, M. R.; Niemczyk, M. P.; Johnson, D. G.; Svec, W. A.; Minsek, D. W. *Tetrahedron* **1989**, *45*, 4785−806.
(25) Johnson, D. G.; Niemczyk, M. P.; Minsek, D. W.; Wiederrecht, G. P.; Svec, W. A.; Gaines, G. L., III; Wasielewski, M. R. *J. Am. Chem. Soc.* **1993**, *115*, 5692−701.
(26) Wiederrecht, G. P.; Watanabe, S.; Wasielewski, M. R. *Chem. Phys.* **1993**, *176*, 601−14.
(27) Osuka, A.; Marumo, S.; Mataga, N.; Taniguchi, S.; Okada, T.; Yamzaki, I.; Nishimura, Y.; Ohno, T.; Nozaki, K. *J. Am. Chem. Soc.* **1996**, *118*, 155−167.
(28) Osuka, A.; Mataga, N.; Okada, T. *Pure Appl. Chem.* **1997**, *69*, 797−802.
(29) Kumar, K.; Lin, Z.; Waldeck, D. H.; Zimmt, M. B. *J. Am. Chem. Soc.* **1996**, *118*, 243−244.

systems that have anthracene donors and dimethyl maleate acceptors at opposite ends of the C-shaped molecule. Entrapment of benzonitrile in the cleft results in a much larger electron-transfer rate than does the more difficult to reduce acetonitrile. This suggests that the lower energy D^+-B^--A virtual state involving benzonitrile results in a faster rate of electron transfer via the superexchange mechanism.

In the work presented here new D−B−A molecules based on a 4-aminonaphthalene-1,8-imide (ANI) donor and a 1,8:4,5-naphthalenediimide (NI) acceptor have been synthesized to study the influence of bridging group energetics and orbital symmetry on the formation of D^+-B-A^-. These particularly simple structures are prepared from building blocks that lend themselves readily to such studies.[30−34] Synthetic details are provided in the Supporting Information. In **1a** and **1b** the 1,4-phenyl bridges between ANI and NI are substituted at the 2 and 5 positions with methyl or methoxy groups (diX), respectively. These substituents alter the energies of the highest occupied and lowest unoccupied molecular orbitals (HOMO and LUMO, respectively) of the bridging groups without changing other significant factors such as the donor−acceptor distance and orientation which affect electron-transfer rates. In addition, the π system of the bridge is constrained by steric interactions to an orientation that is nearly orthogonal to those of ANI and NI, which places the π systems of the donor and acceptor in the same plane. The molecular triads **2a** and **2b** are analogous to the dyads, except that an additional electron donor moiety, 4-methoxyaniline (MeOAn), is attached to ANI via a piperazine spacer. These compounds were synthesized to study the effects of bridge energetics on charge separation when its mechanism involves the initial migration of positive charge away from the bridge. Excitation of ANI within **2a** and **2b** results in rapid electron transfer from 4-methoxyaniline to ^{1}*ANI to yield $MeOAn^+$-ANI^--diX-NI. Thus, the initial CS step within triads **2a** and **2b** is the reduction of ^{1}*ANI, whereas that for dyads **1a** and **1b** is the oxidation of ^{1}*ANI. Formation of the $MeOAn^+$-ANI-diX-NI^- state within **2a** and **2b** occurs via a secondary charge shift reaction.

Compounds **3a** and **3b** were synthesized to determine what role, if any, the bridge itself plays in quenching the ^{1}*ANI excited state, and to better understand the behavior of the D−B−A dyads. They consist of identical donor and bridge moieties, but replace NI with a terminal naphthalene-1,8-monoimide (NMI), which cannot be reduced by ^{1}*ANI; however, its presence does provide a substituent effect similar to that of NI on the electronic structure of the phenyl bridge. In an analogous manner, it is possible to study the properties of the B^+-A^- state by substituting NMI for ANI. The reference molecules **4a** and **4b**, which lack the ANI donor, use NMI again to maintain the effect of an imide substituent on the bridge electronic structure.

Results

Steady-State Spectroscopy. The photophysics of the 4-(*N*-piperidinyl)naphthalene-1,8-imide (ANI) chromophore have been characterized previously in detail.[35] The ground-state optical spectrum of ANI in toluene exhibits a broad absorption centered at 398 nm, which possesses about 70% charge-transfer character. The ground-state absorption spectra of the bridged dyads **1a** and **1b** in toluene show the absorption band due to ANI as well as bands due to the NI acceptor at 343, 363, and 382 nm.[36] The lowest energy NI absorption band partially overlaps the blue edge of the ANI charge-transfer absorption band, Figure 1.[30,37] The ground state optical spectra of these compounds are approximately the sum of the spectra of the isolated chromophores, *N*-(*p*-tolyl)-4-(1-piperidinyl)naphthalene-1,8-dicarboximide (ANI) and *N*,*N*′-di-(*n*-octyl)-1,8:4,5-naphthalene-tetracarboxydiimide (NI), respectively, suggesting weak electronic interaction between the ANI and NI moieties in all of these molecules. Increasing the solvent polarity results in no spectral shift of the NI peaks, while the ANI charge-transfer band shifts to 405 nm in butyronitrile (PrCN), further resolving it from the NI vibronic bands. The corresponding ground-state absorption spectra for the triads **2a** and **2b** exhibit analogous behavior.

The charge transfer state of ANI decays radiatively in all solvents, with an emission maximum at 497 nm in toluene. The

Chart 1

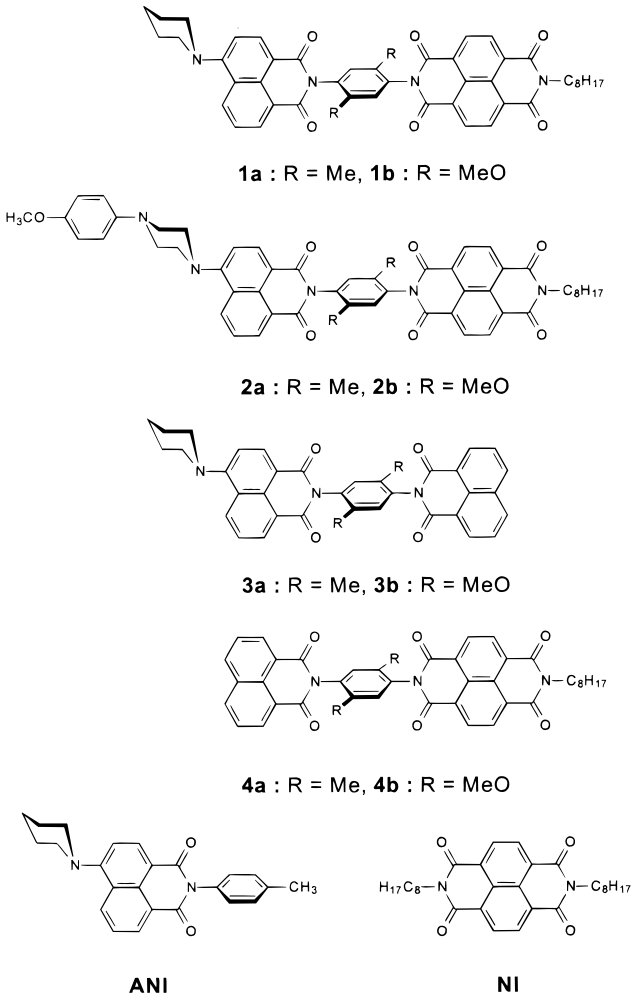

(30) Korol'kova, N. V.; Val'kova, G. A.; Shigorin, D. N.; Shigalevskii, V. A.; Vostrova, V. N. *Russ. J. Phys. Chem.* **1990**, *64*, 206−209.
(31) Alexiou, M. S.; Tychopoulos, V.; Ghorbanian, S.; Tyman, J. H. P.; Brown, R. G.; Brittain, P. I. *J. Chem. Soc., Perkin Trans. 2* **1990**, 837−842.
(32) Dietz, T. M.; Stallman, B. J.; Kwan, W. S. V.; Penneau, J. F.; Miller, L. L. *J. Chem. Soc., Chem. Commun.* **1990**, 367−9.
(33) Debreczeny, M. P.; Svec, W. A.; Wasielewski, M. R. *New J. Chem.* **1996**, *20*, 815−828.
(34) Gosztola, D.; Wang, B.; Wasielewski, M. R. *J. Photochem. Photobiol., A* **1996**, *102*, 71−80.
(35) Greenfield, S. R.; Svec, W. A.; Gosztola, D.; Wasielewski, M. R. *J. Am. Chem. Soc.* **1996**, *118*, 6767−6777.
(36) Adachi, M.; Murata, Y.; Nakamura, S. *J. Phys. Chem.* **1995**, *99*, 14240−14246.
(37) deSilva, A. P.; Gunaratne, H. Q. N.; Habib-Jiwan, J.-L.; McCoy, C. P.; Rice, T. E.; Soumillin, J.-P. *Angew. Chem., Int. Ed. Engl.* **1995**, *34*, 1728−1731.

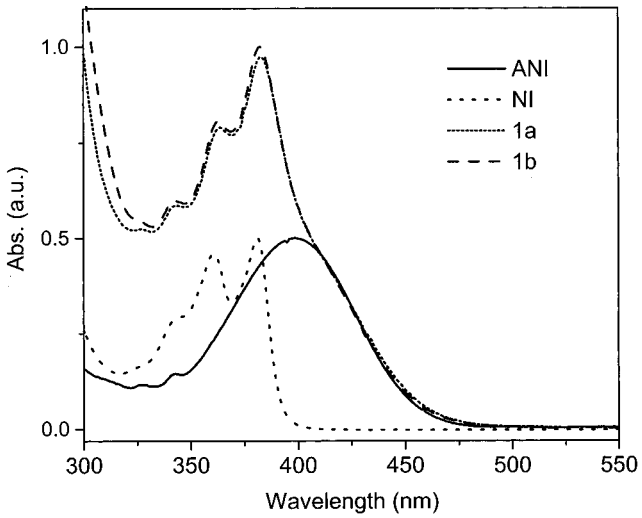

Figure 1. UV−vis absorption spectra of the indicated molecules in toluene.

Table 1. Spectroscopic Properties of the ANI Chromophore

solvent	λ_{abs} (nm)	λ_{em} (nm)	Φ_F	E_S (eV)	τ_f (ns)
toluene	398	497	0.910	2.81	8.5
MTHF	397	514	0.790	2.76	7.5
PrCN	405	530	0.230	2.70	1.5

spectroscopic properties of the isolated ANI chromophore in the solvents toluene, MTHF, and PrCN are given in Table 1. As the polarity of the solvent increases, the emission maximum shifts to red and the fluorescence quantum yield decreases. These effects are consistent with stabilization of the ^{1}*ANI excited state in higher polarity media, due to its charge-transfer character.

The steady-state spectroscopic properties of **3a** and **3b** are listed in Table 2. Compound **3a** exhibits a ground-state absorption spectrum in which the ANI CT absorption feature dominates. A weaker absorption due to NMI appears at 340 nm. The absorption and emission spectra of **3a** are virtually identical to those of ANI and **1a** in all solvents, which shows that NMI has an effect similar to NI on the electronic structure of the donor and bridge. Interestingly, the absorption maximum of ANI within **3b** exhibits a solvent-dependent red shift of 5 to 10 nm relative to both **3a** and ANI itself, which is also reflected in the emission spectra. The quantum yields of **3b** also display solvent-dependent behavior not observed in the isolated chromophores. In toluene and MTHF the fluorescence quantum yields of **3b** are close to that of ANI, but in PrCN the fluorescence quantum yield is quenched significantly relative to that of ANI itself. These observations indicate that an interaction between the donor and bridge occurs, whose magnitude increases with solvent polarity and lowering of the excited-state energy.

The fluorescence emission from ^{1}*ANI is quenched in the presence of nearby electron acceptors. In the case of **1a** this quenching has been shown previously to arise from photoinduced electron transfer from ^{1}*ANI to NI.[35] Fluorescence quantum yields and emission maxima for the D−B−A dyads **1a** and **1b** are given in Table 2. Emission from **1b** is quenched more strongly than that of **1a** in all solvents.

The absorption and emission features of the triads **2a** and **2b** are very similar to those of the dyads, and are dominated by the ANI and NI absorptions. Earlier data obtained for **2a** show that rapid electron transfer occurs from *p*-methoxyaniline to the adjacent ^{1}*ANI excited state, quenching the fluorescence. The fluorescence quenching data for **2b,** Table 2, suggests that the corresponding methoxy-substituted derivative may be undergoing the same reaction.[35] Moreover, the data suggest that the electron-transfer pathways that occur in **2b** are most likely quite different from those that occur in the corresponding dyad, **1b** (vide infra).

Compounds **4a** and **4b** have the structure NMI−B−A where NMI is substituted for ANI, while NI is the isolated 1,8:4,5-naphthalenediimide chromophore substituted at the amide nitrogens with *n*-octyl groups. Excitation within the central vibronic band of NI with 360 nm light results in formation of the ^{1}*NI excited state, whose emission maximum is 406 nm in toluene. In **4a** and **4b** this emission is quenched significantly, which suggests that B^+-A^- may form in these molecules. The fluorescence quantum yields for these compounds are listed in Table 3.

Redox Potentials. AC voltammetry was used to determine the oxidation potentials of the ANI donor and the *p*-dimethoxyphenyl bridge in the D−B−A molecules, Table 4. The value of $E_{ox} = 1.41$ V vs SCE for *p*-dimethoxybenzene obtained in this study agrees reasonably well with the 1.32 V vs SCE reported in the literature,[38] as does $E_{ox} = 1.20$ V for ANI.[35] Compound **1b** undergoes two one-electron oxidations at 1.22 and 1.67 V. Compound **4b**, lacking the ANI donor, undergoes a single one-electron oxidation at 1.63 V. These results show that imide groups bound to the 2 and 5 positions of *p*-dimethoxybenzene increase its oxidation potential by about 0.25 V relative to that of *p*-dimethoxybenzene.

The similarity between the oxidation potentials of the bridge molecules in **1b** and **4b** indicates that the positive change in the oxidation potential of the *p*-dimethoxyphenyl bridge relative to that of *p*-dimethoxybenzene is not due to the presence of the ANI electron donor. There are two possible explanations for this observed change. The imide substituents are somewhat electron withdrawing, and are known to raise the oxidation potentials of other systems.[39] A second possibility is that steric hindrance between the methoxy groups and the oxygen atoms of the imides forces the methoxy groups out of the plane of the bridge phenyl ring, which reduces the conjugation of the oxygen lone pair with the π system of the phenyl, presumably making it more difficult to oxidize. Geometry-optimized AM1 calculations[40,41] predict that in **1b** the average torsional angle that the C−O bonds of the two *p*-dimethoxyphenyl groups make with the π system of the phenyl is 24.5°. This compares with a torsional angle of 8.6° in *p*-dimethoxybenzene. Thus, it is likely that the increased oxidation potential of the *p*-dimethoxybenzene bridge observed in **1b** and **4b** is a combination of steric and electronic effects. The measured redox potentials for the donors and acceptors, as well as those of selected bridge molecules, were used to calculate the ion pair state energies of the various intermediates observed in this study (vide infra).

Time-Resolved Spectroscopy. Ultrafast transient absorption spectroscopy allows for direct observation of intermediate states formed during photoinduced charge separation reactions. Transient absorption measurements on the reference molecules **3a** and **3b** in toluene display two features, illustrated for **3a** in Figure 2a. The positive ΔA at 450 nm is the ^{1}*ANI excited-

(38) Meites, L.; Zuman, P.; Scott, W. J.; Campbell, B. H.; Kardis, A. M. *Electrochemical Data*; John Wiley and Sons: New York, 1974; Vol. 1.
(39) Wiederrecht, G. P.; Svec, W. A.; Wasielewski, M. R. *Springer Ser. Chem. Phys.* **1994**, *60*, 452−3.
(40) Dewar, M. J. S.; Zoebisch, E. G.; Healy, E. F.; Stewart, J. J. P. *J. Am. Chem. Soc.* **1985**, *107*, 3902−9.
(41) Ion pair distances were estimated from structures calculated using the MM+ force field and AM1 MO calculations performed within Hyperchem V5.01a (Hypercube, Waterloo Ontario).

Table 2. Steady State Spectroscopic Properties of Bridged Compounds **1**, **2**, and **3**

	toluene				MTHF				PrCN			
compd	λ_{abs}	λ_{em}	Φ_F	τ_f (ns)	λ_{abs}	λ_{em}	Φ_F	τ_f (ns)	λ_{abs}	λ_{em}	Φ_F	τ_f (ns)
1a	384	500	0.168		379	523	0.070		383	533	0.044	
1b	384	496	0.012		378	511	0.015		383	530	0.015	
2a	384	499	0.006		378	500	0.004		383	497	0.002	
2b	384	499	0.007		379	501	0.004		383	498	0.002	
3a	399	497	0.911	10.0	398	510	0.807	7.1	406	531	0.213	1.82
3b	404	501	0.928	6.3	403	515	0.684	6.2	416	536	0.019	0.17

Table 3. Spectroscopic Properties of NI and X−B−A Reference Compounds in Toluene

	toluene				
compd	λ_{abs}	λ_{em}	Φ_f	τ_{CS} (ps)	τ_{CR} (ps)
NI	382, 362, 342	406	0.05		
4a	381, 362, 340	405	0.0005	0.63	125
4b	381, 362, 340	406	0.0006	0.63	114

Table 4. Redox Potentials (vs SCE)

compd	E_{ox1} (V)	E_{ox2} (V)	E_{red} (V)
NI			−0.53
ANI	1.20		−1.40
p-dimethoxybenzene	1.41		
1b	1.20	1.67	
4b	1.63		

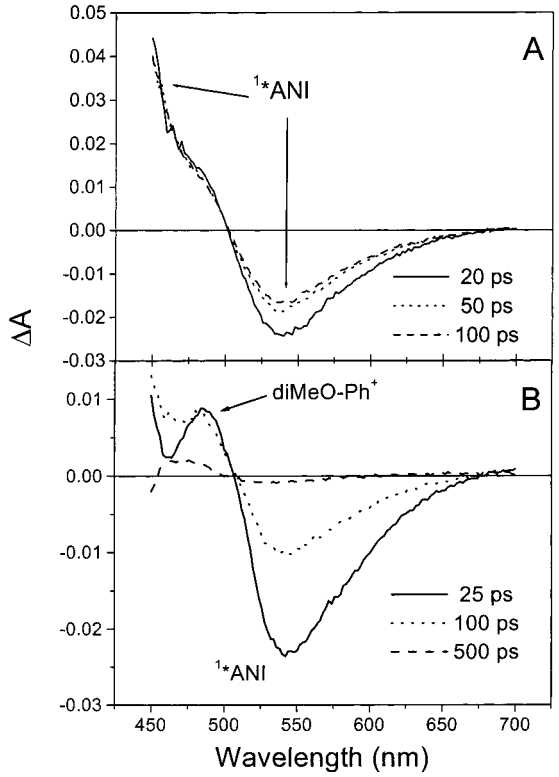

Figure 2. Transient absorption spectra of (A) **3a** in toluene and (B) **3b** in PrCN at the noted times following a 400 nm, 130 fs laser flash.

state absorption, while the negative Δ*A* at 535 nm is due to stimulated emission from this state. Both features appear in **3a** and **3b** within the 180 fs instrument response function. As the solvent polarity increases, the stimulated emission red shifts, mirroring the steady-state spectra. While no electron transfer occurs within either **3a** or **3b** in toluene and MTHF, the fluorescence for **3b** in PrCN is quenched and its excited-state lifetime is much shorter. For **3b** in PrCN the *p*-dimethoxyphenyl bridge is a good enough electron donor to reduce ^{1}*ANI. The

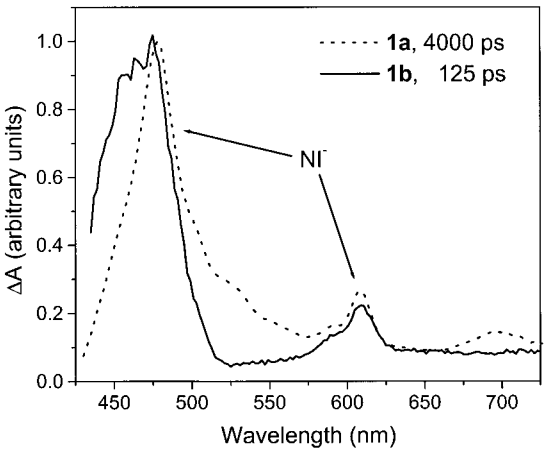

Figure 3. Comparison of the transient absorption spectra of **1a** and **1b** in toluene at the indicated times following a 400 nm, 130 fs laser flash.

transient absorption spectrum of **1b** in PrCN, Figure 2b, exhibits a peak at 485 nm characteristic of the *p*-dimethoxybenzene radical cation.[42]

The electron-transfer dynamics of the D−B−A compounds **1a** and **1b** were studied in several solvents to directly determine their rates of charge separation and recombination. Upon excitation in toluene their transient spectra display an absorption band at 450 nm and stimulated emission at 535 nm. The spectra of **1a** and **1b** both evolve with time to reveal absorption bands at 480 and 607 nm characteristic of NI^-.[35] Figure 3 shows the signals from **1a** and **1b** in toluene at the times at which their maximum ion pair populations occur. The spectrum of **1b** shows a residual absorption at 450 nm from the ^{1}*ANI excited state and the intense absorption band due to the NI radical anion (λ_{max} = 475 nm, ϵ = 28000 l·M^{-1}). The dielectric constant of the solvent significantly affects the electron-transfer rates. Monitoring the formation and decay of Δ*A* for NI^- allows for direct determination of the CS and CR time constants. The CS and CR rates for the D−B−A dyads listed in Table 5 show that in toluene these processes occur much faster in **1b** than in **1a**. However, this difference diminishes in higher polarity media and converges to a common set of values.

The transient absorption spectra of **2a** and **2b** in toluene are shown in Figure 4. Following excitation, a broad absorption band appears near 500 nm, which is characteristic of the ANI radical anion and the MeOAn cation radical.[43,44] This spectral feature is indicative of the formation of the $MeOAn^+$-ANI^--diX-NI state, and evolves over several hundred picoseconds to a spectrum characteristic of $MeOAn^+$-ANI-diX-NI^-, with peaks at 480 and 607 nm. The time constants for each of these

(42) Shida, T. *Electronic absorption spectra of radical ions*; Elsevier: Amsterdam, 1988.

(43) Kimura, K.; Yoshinaga, K.; Tsubomura, H. *J. Phys. Chem.* **1967**, *71*, 4485−4491.

(44) Hester, R. E.; Williams, K. P. J. *J. Chem. Soc., Perkin Trans. 2* **1982**, 559−563.

Table 5. Electron Transfer Time Constants for Compounds **1** and **2**

	toluene			MTHF			PrCN		
compd	τ_{CS1} (ps)	τ_{CS2} (ps)	τ_{CR} (ps)	τ_{CS1} (ps)	τ_{CS2} (ps)	τ_{CR} (ps)	τ_{CS1} (ps)	τ_{CS2} (ps)	τ_{CR} (ps)
1a	1500		170000	516		2410	86		456
1b	47		119	152		594	85		350
2a	8	430	230000	2	370	1350	1.5		4
2b	8	600	25000	2	95	170	1		10

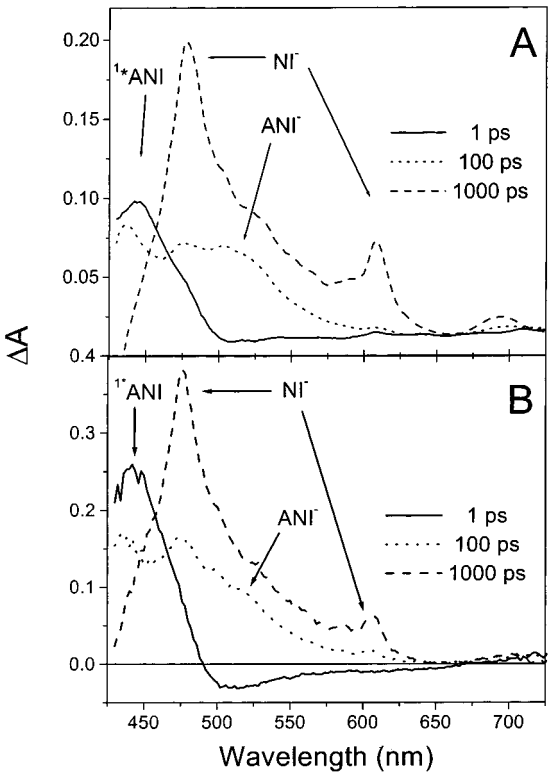

Figure 4. Transient absorption spectra of (A) **2a** and (B) **2b** in toluene at the noted times following a 400 nm, 130 fs, laser flash.

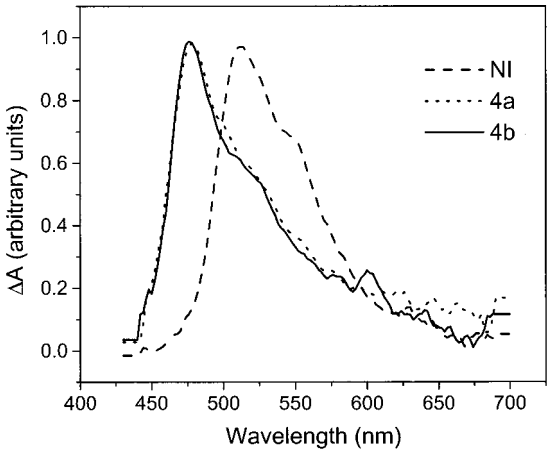

Figure 5. Comparison of the transient absorption spectra for **4a** and **4b** in toluene at 25 ps following a 360 nm, 130 fs laser flash.

electron-transfer events are listed in Table 5. Interestingly, the kinetics of the charge shift reaction MeOAn$^+$-ANI$^-$-diX-NI → MeOAn$^+$-ANI-diX-NI$^-$ show only a weak dependence on the substituent X.

The reference compounds NI, **4a,** and **4b** have no significant ground-state absorption at 400 nm, so that transient absorption data were acquired by direct excitation of the NI component at 360 nm. The excited-state spectrum of ^{1}*NI has an asymmetric absorption centered at 510 nm, Figure 5, which decays with τ = 3 ns. This lifetime is significantly reduced in **4a** and **4b**. In each of these compounds, the transient spectra evolve rapidly in <1 ps to yield the absorption spectrum characteristic of NI$^-$, Figure 5. This can be attributed to electron transfer from the adjacent phenyl ring to ^{1}*NI, forming the ion pair NMI−B$^+$−A$^-$. The lifetimes of these ion pair states are listed in Table 3. It should be noted that the ion pairs formed within **4b** and **1b** have nearly identical CR rates, which suggests that the same charge separated state may be formed in both compounds.

Discussion

Energetics. The lowest excited-state energies of ANI in toluene, MTHF, and PrCN are listed in Table 1. Greenfield et al. showed that ^{1}*ANI possesses about 70% charge-transfer character.[35] Using this fact and the solvent dependence of the energy of this state, electron transfer from ^{1}*ANI to NI can be treated as a charge shift reaction. Energy changes due to solvation of the charge distribution are taken into account by the solvent dependence of the excited-state energy of ^{1}*ANI. Thus, to a reasonable approximation the calculation of the ion pair energy depends only on the donor−acceptor distance, and differences in redox potentials. Using this model, no additional solvation terms are material to the calculation, wherein the use of these terms in the dielectric continuum model of Weller[45] consistently underestimates the degree to which a polarizable solvent, such as toluene, stabilizes an ion pair.[46] Using the spectroscopic data for ^{1}*ANI and the redox potentials of the donor and acceptor, the ion pair state energy of ANI$^+$-diMe-NI$^-$ in toluene is 2.42 eV.[35] The energy of the ANI$^+$-diMeO−NI$^-$ ion pair is also 2.42 eV in toluene because the donor, acceptor, and ion pair distance are identical. The energies of the ion pair states involving the bridge molecules, ANI$^+$−B$^-$−NI and ANI−B$^+$−NI$^-$, in toluene were calculated relative to the energy of ANI$^+$-diMe-NI$^-$ using the relationship

$$\Delta G_{IP2} = \Delta G_{IP1} + |E_2 - E_1| + \frac{e^2}{\epsilon_s}\left(\frac{1}{r_{IP1}} - \frac{1}{r_{IP2}}\right) \qquad (1)$$

where ΔG_{IP1} and r_{IP1} are the ion pair energy and distance, respectively, in compound **1a**, ΔG_{IP2} and r_{IP2} are the ion pair energy and distance,[41] respectively, for ANI$^+$−B$^-$−NI or ANI−B$^+$−NI$^-$, E_2 is the oxidation or reduction potential of the bridge molecule, E_1 is the oxidation potential of ANI or the reduction potential of NI, e is the electronic charge, and ϵ_s is the static dielectric constant of the solvent. The ion pair energies in MTHF and PrCN were calculated directly using the oxidation and reduction potentials of the donor and acceptor, respectively, and the Coulomb stabilization of the ion pair

$$\Delta G_{IP} = E_{OX} - E_{RED} - \frac{e^2}{\epsilon_s \cdot r_{DA}} \qquad (2)$$

(45) Weller, A. Z. *Z. Phys. Chem.* **1982**, *133*.
(46) Warman, J. M.; Smit, K. J.; Jonker, S. A.; Verhoeven, J. W.; Oevering, H.; Kroon, J.; Paddon-Row, M. N.; Oliver, A. M. *Chem. Phys.* **1993**, *170*, 359−380.

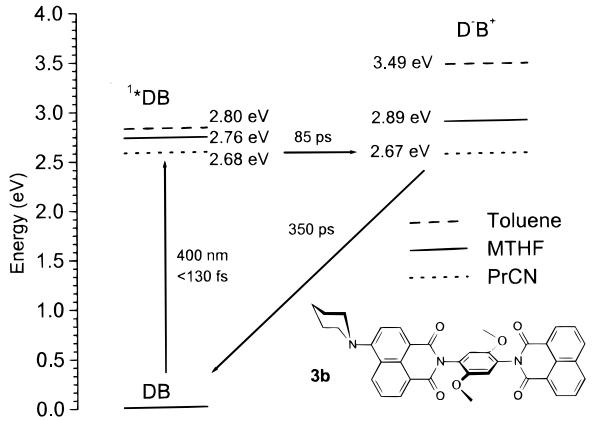

Figure 6. Energy levels for **3b** in the indicated solvents.

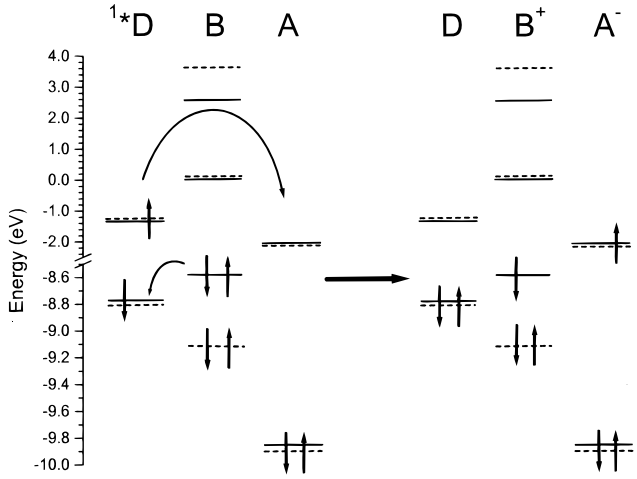

Figure 7. Energy level diagram featuring the frontier molecular orbitals of D, B, and A within **1a** (- - -) and **1b** (—). All orbitals above 2.0 eV are σ orbitals, while those below 2.0 eV are π orbitals.

where r_{DA} is the distance[41] between the separated ions. The corresponding values of the free energies of CS and CR are

$$\Delta G_{CS} = \Delta G_{IP} - E_S \tag{3}$$

where E_S is the lowest excited-state energy of the donor, and

$$\Delta G_{CR} = -\Delta G_{IP} \tag{4}$$

The calculated CS free energies predict that electron transfer is thermodynamically possible in all three solvents for all compounds having both the ANI donor and the NI acceptor. A selection of these data relevant to the arguments discussed below are presented in Figures 6 and 8.

Photoinduced Charge Separation and Recombination Mechanisms. Model compounds **3a** and **3b** contain the terminal NMI group that thermodynamically cannot be reduced by ^{1}*ANI. In toluene and MTHF both compounds have fluorescence quantum yields comparable to or greater than that of ANI alone, suggesting that electron transfer does not occur. In the polar solvent PrCN, however, the fluorescence quantum yield of **3b** is reduced by more than an order of magnitude relative to those of ANI and **3a**. This suggests the possibility of bridge-to-donor electron transfer, forming ANI$^-$-diMeO$^+$-NMI. The energies of this state in toluene, MTHF, and PrCN were calculated using eq 2, the reduction potential of ANI, and the oxidation potential of the *p*-dimethoxyphenyl bridge, Figure 6. The calculations indicate that in toluene and MTHF the ANI$^-$-diMeO$^+$-NMI ion pair state lies well above the excited state of the ANI chromophore, while in PrCN the ion pair and excited state are nearly isoenergetic. The transient spectrum of **3b** in PrCN (Figure 2b) supports this mechanism. A peak at 485 nm, which is resolved from the short-lived absorption of ^{1}*ANI at 450 nm, appears in neither **3a** in PrCN nor **3b** in MTHF, where the D$^-$—B$^+$ state is not energetically favored. Thus, the observed 485 nm peak is attributed to the *p*-dimethoxyphenyl radical cation,[42] whose formation is strictly dependent on solvent polarity.

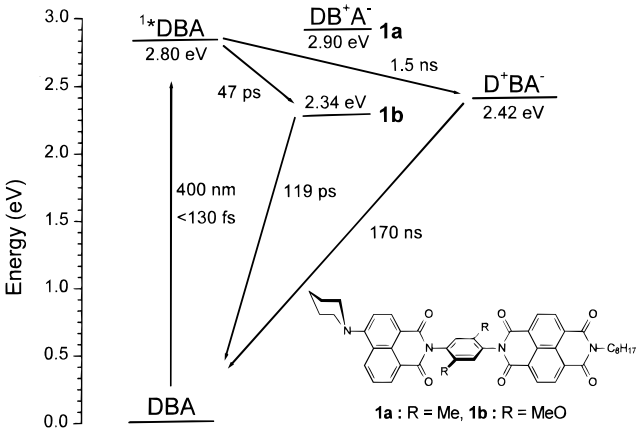

Figure 8. Energy levels for **1a** and **1b** in toluene.

The dyads **1a** and **1b** are analogous to the model compounds **3a** and **3b** except that the NI electron acceptor in **1a** and **1b** can be reduced by ^{1}*ANI. These compounds demonstrate that methoxy substituents on the phenyl bridge dramatically increase both the CS and CR rates relative to those observed for the dimethyl-substituted phenyl bridge. Again, solvent polarity plays a major role in determining the mechanisms of CS and CR. Previous work has demonstrated that electron transfer in **1a** occurs predominantly through the σ-bonded framework of the bridge in all solvents.[35] The data are consistent with small donor—bridge and bridge—acceptor electronic couplings due to the orthogonal arrangement of the bridge relative to both the donor and the acceptor. In low polarity media this superexchange mechanism results in slow rates for both CS and CR, while both processes become faster in higher polarity media.

In toluene the CS and CR rates for **1b** increase by factors of 32 and 1400, respectively, over those for **1a**, despite the seemingly small electronic coupling due to the orthogonal bridging group. If electron transfer in **1b** also occurs predominantly through the σ-bonded framework of the bridge, then one might expect an enhancement of the electron-transfer rates due to the inductive electron withdrawing effect of the methoxy groups on the bridge. The electronic coupling matrix element for an electron-transfer reaction mediated by a superexchange interaction involving the bridge is given by

$$V_{DA} = \frac{V_{DB}V_{BA}}{\Delta E} \tag{5}$$

where V_{DB} and V_{BA} are the electronic coupling matrix elements for the donor—bridge and bridge—acceptor interactions, and ΔE is the vertical energy difference between the potential energy surfaces of the donor and bridge states.[15] Given that the electron-transfer rate constant $k_{DA} \propto V^2_{DA}$, and assuming that V_{DB} and V_{BA} are similar for **1a** and **1b**, the ratio of electron-transfer rate

constants k_{1b}/k_{1a} can be expressed as

$$\frac{k_{1b}}{k_{1a}} = \frac{\Delta E_{1a}^{\,2}}{\Delta E_{1b}^{\,2}} \qquad (6)$$

It is not possible to obtain the relevant energies of the σ orbitals of B to include in eq 6 using electrochemical data because the LUMO of B, which would accept the electron, is a π orbital. Even the energy of the π symmetric LUMO of benzene itself is difficult to obtain from electrochemical data because its reversible thermodynamic reduction potential is very negative, $E_{1/2} = -3.4$ V vs SCE.[47] As an alternative, the orbital energies of the frontier MOs localized on D, B, and A within **1a** and **1b** were calculated using the AM1 model and are shown in Figure 7. The calculations show that the lowest energy unoccupied orbitals in both compounds are π orbitals localized on A. The lowest unoccupied π orbitals localized on B in **1a** and **1b** are 1.4 and 1.2 eV above the HOMO of D, respectively, while the corresponding σ orbitals of B are 5.0 and 3.9 eV above the HOMO of D. This is the usual energy ordering for D−B−A molecules. The orientation of ANI relative to the bridge suggests that electron transfer from the HOMO of ANI to NI involves the σ orbitals of B in a superexchange interaction. Using the energy difference between the HOMO of ANI and the lowest unoccupied σ orbital of B for **1a** and **1b** in eq 6 yields $k_{1b}/k_{1a} = 1.6$, while the experimentally determined ratio is 32. Thus, the inductive effect of the methoxy groups and a superexchange mechanism that uses the σ bonds of the bridge cannot account for the observed increase in CS and CR rates for **1b** relative to those for **1a**.

On the other hand, if the π orbitals of the bridge are involved in the electron transfer, k_{1b}/k_{1a} should be influenced significantly by replacing the methyl substituents on the phenyl bridge with the more π electron-releasing methoxy substituents. Experimentally, *p*-dimethoxybenzene is easier to oxidize than *p*-dimethylbenzene by about 0.4 V,[48] which is reflected in the ordering of the energies of the calculated HOMOs for the bridges and ANI in **1a** and **1b**, Figure 7. In **1a,** the HOMO is localized on ANI, while the next highest occupied orbital (HOMO-1) is localized on the *p*-dimethylphenyl bridge. The energy gap between these two orbitals is 0.3 eV. The situation is reversed in **1b** where the HOMO is localized on the *p*-dimethoxyphenyl bridge, and the energy difference between it and the highest occupied orbital localized on ANI is 0.3 eV. Notwithstanding the fact that these calculations were made on isolated molecules in the gas phase, these results predict that bridge-to-donor electron transfer is possible in **1b**, but not in **1a**. Thus, ^{1}*D−B−A may undergo a double electron transfer in which electron transfer from ^{1}*D to A occurs concomitant with electron transfer from B to ^{1}*D, as shown in Figure 7. The energy of the hypothetical intermediate D−B$^+$−A$^-$ state in the CS reactions of **1a** and **1b** can be calculated using eq 1. The results of this calculation for **1a** and **1b** in toluene are shown in Figure 8. The D−B$^+$−A$^-$ state in **1a** is higher in energy than D$^+$-B−A$^-$, while the energy of the D−B$^+$−A$^-$ state in **1b** lies below that of D$^+$−B−A$^-$ by 0.06 eV as well as significantly below that of ^{1}*D−B−A. These data show that the reaction ^{1}*D−B−A → D−B$^+$−A$^-$ is thermodynamically possible in **1b**.

While thermodynamic arguments favor the formation of a D−B$^+$−A$^-$ state within **1b**, the rapid formation of this state requires an electronic interaction that couples both the bridge to the donor and the donor to the acceptor. In addition, these two electron-transfer processes must be coupled to each other, otherwise electron transfer from ^{1}*D to A that uses the LUMO of the bridge would be rate limiting. The highly CT nature of ^{1}*ANI may promote such coupling, as visualized in Figure 9. The positive charge residing in the lone pair orbital of the amine nitrogen within ^{1}*ANI has a convenient route to the π-system of the bridge via σ orbitals of the aryl C−H bonds of the naphthalene-1,8-imide and the lone pair orbitals of the carbonyl groups. The negative charge of the CT state, which resides primarily in the π-symmetric orbitals of the imide group, likewise can undergo electron transfer directly to the π orbital of NI. Interestingly, this mechanism is observed only in toluene, while the difference in both the CS and CR rates between dyads **1a** and **1b** is less pronounced in MTHF, and nearly absent in PrCN. This is a consequence of the fact that in both MTHF and PrCN the D−B$^+$−A$^-$ state within both **1a** and **1b** is higher in energy than the corresponding D$^+$−B−A$^-$ state and the electron transfer proceeds via the conventional superexchange mechanism.

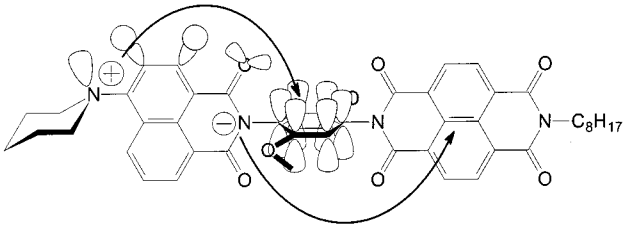

Figure 9. Proposed orbital interactions for the double electron-transfer mechanism.

This mechanistic picture is further supported by examination of the CS dynamics in the triads **2a** and **2b**. As previously mentioned, the fundamental difference between the dyads and triads centers on the initial electron-transfer reaction; in the dyads ^{1}*ANI acts as an electron donor, whereas in the triads, it functions as an electron acceptor. In the triads, ANI is reduced in the initial photoinduced electron transfer to yield MeOAn$^+$-ANI$^-$-diX-NI. In this intermediate a full negative charge resides on the naphthalene-1,8-imide ring of ANI, while the positive charge is moved farther away and resides on the oxidized *p*-methoxyaniline donor. Thus, only the charge shift from ANI$^-$ to NI occurs. The coplanar orientation of the π systems of ANI and NI within **2a** and **2b** suggests that only direct interactions of these orbitals and/or participation of the σ orbitals of the phenyl bridge should be important in transferring the electron from ANI$^-$ to NI. If this model is correct, changing the substituents on the phenyl bridge should have a minor impact on the charge shift rate constant. The spectral (Figure 4) and kinetic (Table 5) data both show that there is no significant difference between the dynamics observed in **2a** and **2b** in any solvent. These data lend further support to the arguments presented earlier that the inductive effect of the methoxy groups on the bridge molecule have only a small impact on electron-transfer rates that employ the σ-bonded pathway through the bridge. Thus, the unusual double electron-transfer mechanism proposed for **1b** depends primarily on the energy and symmetry-dependent electronic interaction between the HOMO of ^{1}*ANI and that of the *p*-dimethoxyphenyl bridge.

Additional support for the double electron-transfer mechanism in **1b** is presented by transient absorption data on the reference compounds **4a** and **4b**. These systems lack the ANI electron donor and thus present the possibility of forming the B$^+$−A$^-$ state independent of the production of ^{1}*ANI. If this state is formed in the dyad **1b**, then identical CR rates should be

(47) Mortensen, J.; Heinze, J. *Angew. Chem.* **1984**, *96*, 64−65.
(48) Howell, J. O.; Goncalves, J. M.; Amatore, C.; Klasinc, L.; Wightman, R. M.; Kochi, J. K. *J. Am. Chem. Soc.* **1984**, *106*, 3968−3976.

observed for **1b** and **4b** in toluene. As noted previously, when the **NI** chromophore is photoexcited with 150 fs, 360 nm laser flashes, the transient spectrum evolves rapidly with time to show the excited state with an asymmetric band centered at 520 nm, Figure 5. However, in **4a** and **4b** identical excitation shows the presence of NMI-diX^+-NI^-. The most likely mechanism by which this ion pair forms is electron donation from the adjacent phenyl to ^{1}*NI. This reaction occurs in <1 ps in both in **4a** and **4b**, Table 3. The NMI-diMe^+-NI^- state undergoes CR to the ground state with $\tau = 50$ ps, while the NMI-diMeO^+-NI^- ion pair decays with $\tau = 114$ ps. This latter time constant agrees very well with the $\tau = 119$ ps decay observed for the ANI-diMeO^+-NI^- ion pair proposed to form in **1b**.

Conclusions

Addition of π electron-donating methoxy groups to the bridge of the ANI-diX-NI molecule increases the rates of charge separation and recombination relative to those of the corresponding dimethyl-substituted bridge. The effect is particularly strong in toluene and decreases as the solvent polarity increases. A mechanism consistent with the observed spectroscopic and kinetic behavior is the formation of a charge-separated state ANI-diMeO^+-NI^- via a double electron transfer mechanism that is somewhat analogous to Dexter energy transfer. This mechanism depends critically on the orbital energies and symmetries of the donor relative to those of the bridge. In polar media the energies change sufficiently to return the system to a normal ET mechanism in which electron transfer occurs by means of bridge-mediated superexchange involving the virtual D^+-B^--A state. These observations suggest that the scope of mechanistic possibilities for bridge-mediated electron transfer within organic molecules is very broad, and that given a set of appropriate conditions, unusual mechanisms can strongly dominate the overall electron-transfer reaction.

Experimental Section

All solvents used were either HPLC or spectrophotometric grade except for THF and MTHF. The latter two were distilled over lithium aluminum hydride prior to use. The synthesis and characterization of the new molecules studied in this paper are given in the Supporting Information.

The femtosecond transient absorption apparatus for time-resolved measurements has been described in detail elsewhere.[49] Transient lifetimes of longer than 5 ns were determined using a 10-Hz Nd:YAG laser system. The frequency-tripled output of the Nd:YAG laser (355 nm, ~7 ns) was focused in a pressure cell with 100 PSI H_2, and the Raman line at 416 nm was used to excite the sample and could be blocked by a computer-controlled shutter. The probe light was generated by a xenon flashlamp (EG&G) driven by a homemade circuit, and detected with a Hamamatsu R928 photomultiplier tube with only four dynodes connected. Typically, 10 laser shots each with the pump beam on and pump beam off were averaged by a LeCroy 9384 digital oscilloscope and sent to a computer. Lifetimes of up to 50 μs could be determined with this apparatus. Samples had an optical density of 0.2−0.4 in a 1-cm cuvette. All samples were deoxygenated by bubbling with N_2 for 10 min prior to the experiment.

Absorption measurements were made on a Shimadzu spectrometer (UV-1601), and fluorescence measurements were made on a single-photon-counting fluorimeter (PTI), exciting at 400 or 340 nm. Samples for quantum yield measurements had absorptions of 0.1 ± 0.05 at the excitation wavelength. Quantum yields for 400 nm excitation were determined by comparison to ANI ($\varphi_F = 0.91$), while samples excited at 340 nm were determined by comparison to pyrene ($\varphi_F = 0.7$).

Electrochemistry was performed using a model 173 potentiostat, a model 179 digital coulometer, and a model 175 universal programmer, all from Princeton Applied Research. A small AC signal was applied on top of the voltage sweep using an Ithaco Dynatrac 391 lock-in amplifier, and the response was plotted. All AC voltammetry was performed in 0.1 M tetra-*n*-butylammonium perchlorate in twice-distilled PrCN using a platinum working electrode, a platinum mesh counter electrode, and a saturated calomel reference electrode (SCE).

Acknowledgment. This work was supported by the National Science Foundation (CHE-9732840). The authors also thank Dr. Martin Debreczeny for carrying out preliminary experiments in this study.

Supporting Information Available: The synthesis and characterization of all new molecules (PDF). This material is available free of charge via the Internet at http://pubs.acs.org.

JA001298W

(49) Lukas, A. S.; Miller, S. E.; Wasielewski, M. R. *J. Phys. Chem. B* **2000**, *104*, 931−940.